

Heat of Fusion of the Local Equilibrium of Melting of Isotactic Polypropylene[†]

R. Androsch*[‡] and B. Wunderlich[§]

Institute of Material Science, Martin-Luther-University Halle-Wittenberg, Geusaer Str., 06217 Merseburg, Germany, and Department of Chemistry, The University of Tennessee, Knoxville, Tennessee 37996-1600, and Chemical and Analytical Sciences Division, Oak Ridge National Laboratory, Oak Ridge, Tennessee 37831-6197

Received June 29, 2001

Revised Manuscript Received August 20, 2001

Introduction

Temperature-modulated differential scanning calorimetry (TMDSC) is a useful tool to measure the apparent, reversible heat capacity in the absence of nonlinear, irreversible processes. This condition is best reached using the quasi-isothermal mode in which one can delay the measurement until any slow, irreversible processes such as annealing, crystallization, or melting are completed and a local, structural equilibrium has been achieved.¹ If the measured, apparent, reversible heat capacity is still larger than the thermodynamic, vibrational heat capacity,² this increase may be caused by (I) the temperature dependence of the concentration of crystal defects,³ (II) an equilibrium melting and crystallization of molecules of sufficiently low mass so that no molecular nucleation is necessary,^{4,5} and (III) the reversible melting, i.e., crystallization and melting of macromolecular segments that do not need molecular nucleation.⁶

Recently, some portion of the observed excess in apparent, reversible heat capacity of isotactic polypropylene (iPP) could be assigned to reversible crystallization and melting.⁷ Up to the beginning of irreversible melting, the thermodynamic heat capacity of iPP is practically fully vibrational, which makes an increase in thermodynamic heat capacity by additional conformational contributions (I) less likely than in polyethylene where such contribution can be seen 150 K below the melting temperature due to the temperature-dependent gauche–trans equilibrium within the crystal. Furthermore, the molar mass of the analyzed sample is far beyond the expected limit for reversible melting and crystallization which for iPP should be about 1500 Da,⁵ so that mechanism (II) is also unlikely. This leaves reversible crystallization and melting as the favored cause to explain the observed excess in the apparent, reversible heat capacity (III).

Thermodynamic reversibility of crystallization and melting in polymers can only be achieved when the barriers for crystal and molecular nucleation do not hinder the transition within the time scale of the experiment.⁸ The requirements are fulfilled if the transition can occur at the surface of an existing crystal under conditions that do not need molecular nucleation. The simplest situation would be that the participating

molecules remain connected to the crystal and therefore avoid the need for renewed molecular nucleation; i.e., after a local equilibrium has been reached, the heating step causes a number of molecules on the lateral surface layers to melt only partially, so that they can recrystallize immediately when the cooling step begins.

The degree of reversible crystallization and melting can be expressed as an apparent heat capacity in terms of the percentage of crystallinity change per kelvin of temperature change.^{9,10} According to the above model, this latent heat contribution to the heat capacity should depend on the chemical structure of the molecule and on the crystal morphology. The chemical structure controls the conformation of the molecule and the intermolecular forces within the crystal and, therefore, the capability of reversible, longitudinal diffusion of the chain (sliding diffusion) and the possible diffusion of chain segments or conformational defects to the fold surface. The temperature-triggered amount of reversible fold-surface crystallization and melting in polyethylene lamellae was observed by small-angle X-ray scattering (SAXS) two decades ago¹¹ and is about twice the amount of the enthalpy-based change in crystallinity if the heat of fusion of bulk polyethylene is used for normalization of the TMDSC enthalpy change.¹² The difference of the reversible crystallinity change obtained by SAXS and by TMDSC was confirmed by wide-angle X-ray scattering (WAXS) and interpreted as a lower heat of the reversible fold-surface crystallization and melting.¹² The strongly decreased reversible difference in enthalpy between the reference states at the fold surface of the homopolymer crystals of polyethylene suggests the description of the reversible effect as an order–disorder process. This description has the advantage to distinguish between true crystallization and melting at the lateral crystal surface with a similar mechanism as also found in irreversible crystallization and melting and the continuous change in defect concentration.

Furthermore, the reversibility of melting of a given molecule is controlled by its crystallization condition. The reversibility of crystallization and melting of poly(ethylene-co-1-octene) significantly increases if the specific lateral surface area of the crystals is enlarged, which suggests an assignment of the reversible transition to the lateral crystal surface and, therefore, a different mechanism than fold-surface melting.¹³ In the case of iPP, it is known that sliding diffusion is much less prevalent than in polyethylene, and as indicated above, the defect concentration within the crystals is negligible when judged by the absolute level of the thermodynamic, vibrational heat capacity. We were able in the prior work to independently vary the specific lateral surface area of the crystals by melt crystallization and by melt quenching followed by long-time annealing. The melt-crystallized crystals were lamellar, while the quenched and annealed crystals were globular with large, lateral specific surface areas. After further annealing during heating, the ultimate melting temperatures of the two samples were constant, indicating that the defect concentrations and crystal thicknesses were, by this time, also similar and that the lateral surface is the location of the reversible melting activity.⁷ In the present paper we attempt to compare the reversible change of crystallinity of iPP probed by tempera-

[†] Presented in part at the 29th Annual Conference of the North American Thermal Analysis Society (NATAS), St. Louis, MO, Sept 24–26, 2001.

[‡] Martin-Luther-University Halle-Wittenberg.

[§] The University of Tennessee and Oak Ridge National Laboratory.

ture-resolved WAXS and TMDSC to check whether the two independent observations refer quantitatively to the same effect and involve the same crystallinity.

Experimental Section

Materials. The material used is a commercial iPP KF 6190 H (Basell), 95–96% isotactic, with molar mass of 373 kg mol^{-1} and polydispersity 6.2.⁷ Thin films of about $200 \mu\text{m}$ thickness were shaped in a hot press (Perkin-Elmer) and subsequently quenched in a mixture of dry ice/ethanol.

TMDSC. The TMDSC was performed with a Mettler-Toledo DSC 820 with the ceramic sensor FRS 5. Cooling was realized by the liquid nitrogen accessory, and the furnace was purged with dry nitrogen at a flow rate of 80 mL min^{-1} . The temperature was calibrated using the onset of melting of indium and zinc, including the tau-lag calibration which corrects the heating rate effect on temperature. The energy flow was calibrated by the heat of fusion of indium. The details of the calculations of the reversing apparent heat capacity from the sawtooth-modulated temperature and the raw heat flow rate are described elsewhere.¹⁴ Quasi-isothermal modulations were done at 373.5, 397.5, and 411.5 K for 180 min with an amplitude of 1.0 K and a period of 240 s. The heat capacity was calibrated using the heat capacity of the melt at 473 and 423 K. After each modulation experiment, the sample was immediately melted at a rate of 10 K min^{-1} to determine the crystallinity, before the next quenching and annealing experiment was started using a new sample. The quasi-isothermal modulation temperature was reached by heating with 10 K min^{-1} .

WAXS. Temperature-resolved WAXS was done on a diffractometer URD 63 (Seifert-FPM), using Ni-filtered $\text{Cu K}\alpha$ radiation. The diffractometer was equipped with a scintillation counter and a vacuum-operated temperature chamber (Paar KG). Intensity data were collected in the reflection mode, using calcium fluoride powder as calibration standard to adjust the position of the sample surface. The temperature at the surface of the sample was checked using contact-less infrared thermometry (nbnElectronics 6T62). The temperature program, i.e., the sample history, the heating rate, and the annealing temperature, was set closely similar to the TMDSC experiments, to permit direct comparison of the data. The annealing time was extended above 180 min to guarantee a metastable global structure, i.e., the absence of irreversible annealing. The irreversible approach to steady state was followed by measuring the intensity of the strong 110 reflection.

Results

TMDSC and DSC. Figure 1 shows the apparent, reversing specific heat capacities of iPP as a function of time at 373.5, 397.5, and 411.5 K, after heating the initially quenched samples from 298 K to the quasi-isothermal modulation temperature with a rate of 10 K min^{-1} . The heat capacities of the melt at 473 and 423 K were used for internal calibration and reveal the typical error of the DSC of less than $\pm 3\%$. This error is mainly caused by limited baseline reproducibility when changing pans. When the pans do not need to be changed, the error reduces to less than $\pm 1\%$.¹⁵ The apparent reversing heat capacity decreases irreversibly during the quasi-isothermal annealing and approaches a metastable equilibrium after several hours, depending on the annealing temperature. The calculation of the excess reversible heat capacity after equilibrium has been reached requires information about the thermodynamic heat capacity at the given crystallinity. For each of the annealing temperatures this crystallinity is determined from the heat of fusion measured by subsequent standard DSC. Figure 2 is a plot of these standard DSC data, which were taken with a heating rate of 10 K min^{-1} . The data reveal a discrete melting

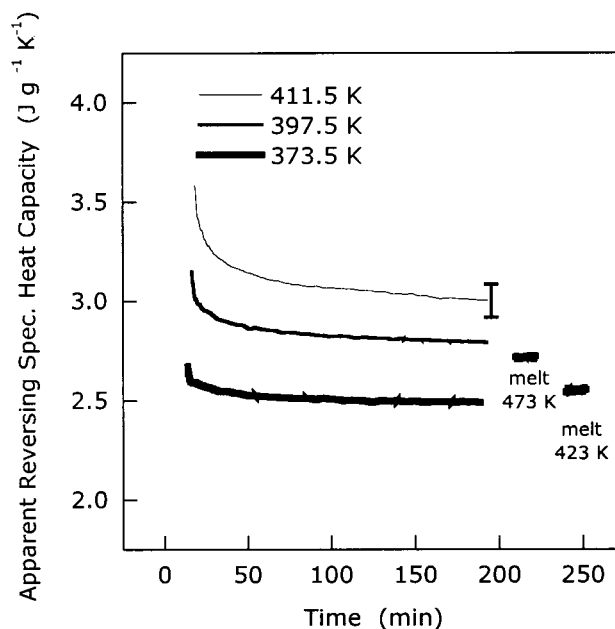


Figure 1. Apparent reversing specific heat capacity of iPP after quenching, followed by reheating with 10 K min^{-1} as a function of time. The data for the melt at 473 and 423 K are used for the internal calibration of the heat capacity.

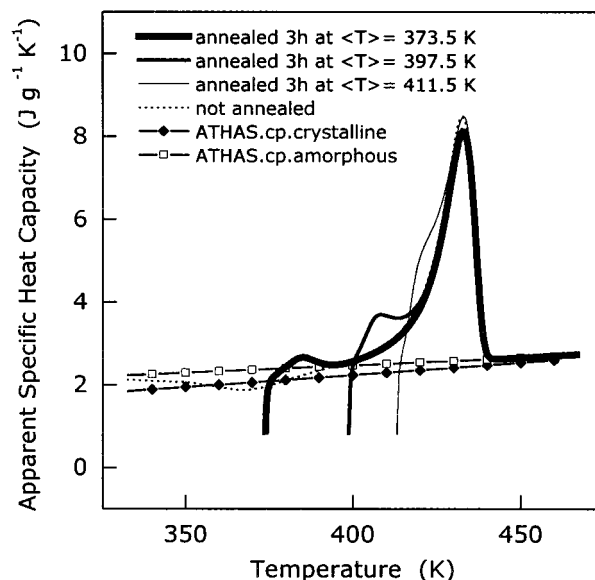
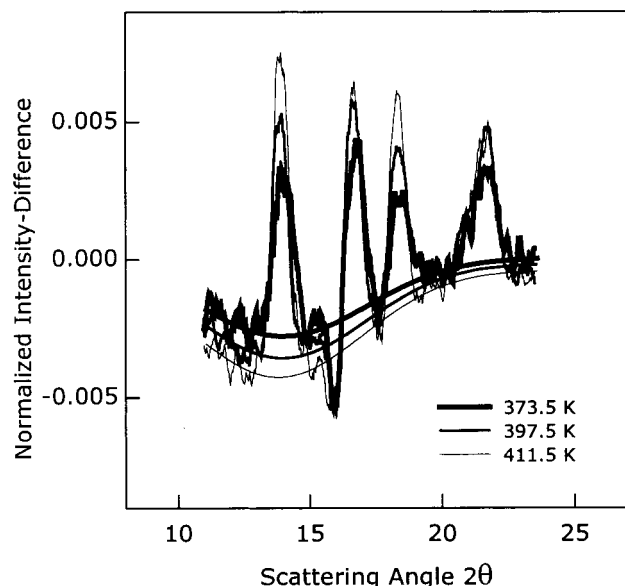


Figure 2. Apparent specific heat capacity during continuous heating of quenched iPP and after annealing at 373.5, 397.5, and 411.5 K.

of reorganized crystals at an about 10–15 K higher temperature than the annealing temperature and a final melting temperature which is not affected by the variation of the annealing temperature. The latter conclusion is derived by comparison with heat capacity data obtained from a not-annealed sample (dotted curve). The crystallinity at the annealing temperatures, which was calculated using temperature-dependent reference enthalpies,² is listed in Table 1, together with the reversing apparent heat capacity, the thermodynamic heat capacity, and the excess heat capacity. The crystallinity at the temperature of annealing is almost independent of the annealing temperature, and the calculated excess heat capacity increases progressively with increasing annealing temperature, in accordance with previous measurements which also contain data

Table 1. Enthalpy-Based Crystallinity and Apparent Reversing Heat Capacity after Quasi-Isothermal Annealing and Thermodynamic Heat Capacity and Excess Heat Capacity as a Function of the Annealing Temperatures

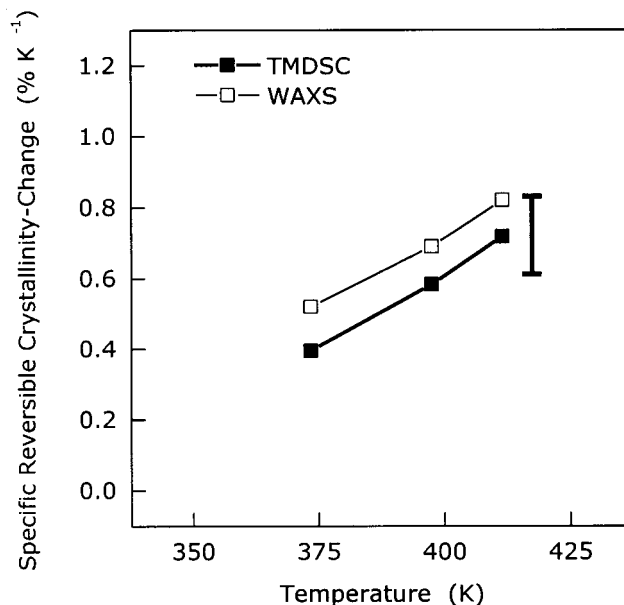
annealing temp (K)	enthalpy-based crystallinity (%)	apparent reversing heat capacity ($\text{J g}^{-1} \text{K}^{-1}$)	thermodynamic heat capacity ($\text{J g}^{-1} \text{K}^{-1}$)	excess heat capacity ($\text{J g}^{-1} \text{K}^{-1}$)
373.5	40	2.49	2.19	0.30
397.5	42	2.79	2.31	0.48
411.5	42	2.98	2.38	0.60

**Figure 3.** Intensity difference $[I(2\theta, T_1) - I(2\theta, T_2)]$ ($T_2 = T_1 + 3 \text{ K}$) of WAXS pattern taken after annealing, normalized to the total crystalline intensity $[I(T_1)]$.

on the melt-crystallized lamellar crystals as well as a characterization of the crystal morphology by AFM and an analysis of the changes on WAXS during isothermal annealing and heating.⁷

WAXS. The temperature-triggered crystallinity change of samples of identical thermal history as used in DSC experiments was measured after completion of irreversible annealing. The irreversible annealing process was monitored using the intensity of the 110 reflection, which revealed a similar kinetics of annealing as observed by the decay of the apparent reversing specific heat capacity (Figure 1). The WAXS crystallinity change on temperature variation is determined as follows: WAXS data, intensity I vs scattering angle 2θ , have been taken between 11° and 23° (2θ) at two different temperatures [T_1 and $T_2 = T_1 + 3 \text{ K}$] within the metastable global equilibrium, achieved by the preceding annealing step. Subsequently, difference patterns $I(2\theta, \text{diff}) [= I(2\theta, T_1) - I(2\theta, T_2)]$ were calculated and normalized to the total crystalline intensity $I(T_1)$. Figure 3 shows the normalized difference pattern calculated from measurements at 372 and 375 K, 396 and 399 K, and 410 and 413 K, i.e., after annealing at 373.5, 397.5, and 411.5 K. The integral of the normalized difference pattern, using a baseline as drawn in Figure 3, gives the crystallinity change per 3 K, normalized to the total crystallinity. Note that the minimum at $\approx 16^\circ$ (2θ) is due to the peak shift by thermal expansion.

The change of crystallinity of the metastable crystals on varying the temperature, as evaluated in the present study is, per definition, reversing. At present a true thermodynamic reversibility of melting can hardly be proved by X-ray scattering methods since it would require continuous data recording vs temperature which exceeds the detector capabilities. For reversibility, the

**Figure 4.** Specific reversible change of crystallinity of the annealed samples of iPP, obtained by TMDSC and WAXS (see Figures 2 and 3).

evolution of crystallinity as a function of temperature must not show any hysteresis, even at the smallest perturbation, which in the case of TMDSC is checked more easily by analysis of the higher harmonics of the Fourier transform of the heat flow rate.^{16,17} Despite these limitations, we will assume, on the basis of our TMDSC data of Figure 1, that the change in crystallinity obtained by WAXS is reversible under the condition of a temperature-modulation amplitude of 1.5 K after extended annealing, albeit the drawback of only limited time resolution of WAXS.

Discussion

Figure 4 summarizes the specific, normalized crystallinity which changes reversibly for the quenched and subsequently annealed samples of iPP as a function of the annealing temperature. The excess heat capacity is recalculated into a reversible change in specific crystallinity by using the heat of fusion of the monoclinic α -polymorph and by normalization to the enthalpy-based crystallinity, to be comparable to the change in the normalized WAXS crystallinity derived from Figure 3. The relative error (standard deviation) is less than $\pm 14\%$ (see the error bar in Figure 4), assuming a maximum relative error of $\pm 3\%$ of the measured heat capacity. The specific reversible change in crystallinity determined by WAXS exhibits a similar error and is at all temperatures $\approx 0.1\% \text{ K}^{-1}$ higher than the value determined by TMDSC. Still, a major cause of the rather small deviation can be suggested in the form of the apparent loss of crystalline intensity by thermal motion of the scattering units within the crystal when raising the temperature.¹⁸ The apparent intensity loss is $(1 - I/I_0) \times 100\% \approx 0.05\% \text{ K}^{-1}$, with $dB/dT = 0.024 \text{ \AA}^2 \text{ K}^{-1}$,¹⁹

and $\sin(\theta)/\lambda = 0.10 \text{ \AA}^{-1}$ (B is the Debye factor, θ the Bragg angle, and λ the wavelength of the X-rays). Note that we consider the intensity loss of $\approx 0.05\% \text{ K}^{-1}$ as the lower limit since the calculation is based on a constant slope dB/dT . The amplitude of thermal vibrations within the crystal is related to the heat capacity of the crystal, which slightly increases in its slope vs temperature.²⁰

The data of Figure 4 show that the specific, reversible changes of crystallinity measured by TMDSC and WAXS agree reasonably well within the estimated error limits, even if no correction for an apparent loss in intensity due to thermal motion in WAXS is performed. The coincidence of the reversibility, measured by WAXS and TMDSC, points to a similar heat of fusion and mechanism of reversible and irreversible melt crystallization. The irreversible crystal growth after nucleation is known, however, to occur preferentially on the lateral crystal surfaces.⁸ The often observed increases of the thickness of lamellae on isothermal annealing (a) by prior melting of thin, unstable crystals which immediately form crystals of increased thickness due to the higher temperature than in the initial crystallization step and (b) by isothermal, longitudinal crystal growth due to the local equilibria at the fold surface we consider to be irreversible processes as well. Both of these processes may contribute to the irreversible decrease of the reversing apparent specific heat capacity seen in Figure 1 and cause the annealing peak during subsequent melting seen in Figure 2.⁹

Reversible crystal growth in the longitudinal chain direction, caused by reversible chain-sliding diffusion within the crystal, a mechanism in the case of polyethylene, i.e., reversible longitudinal crystal growth, seems not to be possible in iPP. Furthermore, the strong mismatch of the reversible change of crystallinity obtained by X-ray methods and TMDSC for polyethylene could only be explained by the assumption that the heat of the reversible fold surface melting is half that of the heat of melting under global equilibrium. Since the fold surface melting occurs at only little lower temperature than equilibrium melting, this must mean that the entropy change which is involved in this process is also much less; i.e., it is not a reversible melting but at best an ordering/disordering. In the present study of reversible crystallization and melting of quenched and annealed iPP we have observed no difference in change of crystallinity by WAXS and TMDSC, and we have therefore no reason to assume a difference in mechanism for reversible and irreversible crystallization. More direct evidence of the constant fold surface in iPP could perhaps be collected by further SAXS analysis of well-defined structures which consist of lamellae, not evident in the present specimens. Nonetheless, the above data strongly support reversible crystallization and melting at the lateral crystal surface, since the result is in

excellent accordance with the recent observation of a drastically decreased reversibility of crystallization and melting if the specific lateral surface area is decreased, as achieved by replacing the globular crystals of this research by laterally extended, melt-grown lamellae as analyzed in our prior publication.⁷

Acknowledgment. The authors gratefully acknowledge experimental support by Ms. H. Müller (Martin-Luther-University Halle-Wittenberg, Institute of Material Science) in infrared thermometry. This work was supported by the Division of Materials Research, National Science Foundation, Polymers Program, Grant DMR-9703692, and the Division of Materials Sciences and Engineering, Office of Basic Energy Sciences, U.S. Department of Energy at Oak Ridge National Laboratory, managed and operated by UT-Batelle, LLC, for the U.S. Department of Energy, under Contract DOE-AC05-00OR22725.

References and Notes

- (1) Boller, A.; Jin, Y.; Wunderlich, B. *J. Therm. Anal.* **1994**, *42*, 307.
- (2) Wunderlich, B. *Thermal Analysis*; Academic Press: Boston, 1990.
- (3) Sumpter, B. G.; Noid, D. W.; Liang, G. L.; Wunderlich, B. *Adv. Polym. Sci.* **1994**, *116*, 27.
- (4) Pak, J.; Wunderlich, B. *J. Polym. Sci., Polym. Phys.* **2000**, *38*, 2810.
- (5) Pak, J.; Wunderlich, B. *Macromolecules* **2001**, *34*, 4492.
- (6) Wunderlich, B.; Mehta, A. *J. Polym. Sci., Polym. Phys.* **1974**, *12*, 255.
- (7) Androsch, R.; Wunderlich, B. *Macromolecules* **2001**, *34*, 5950.
- (8) Wunderlich, B. *Macromolecular Physics*; Academic Press: New York, 1976; Vol. II.
- (9) Androsch, R.; Wunderlich, B. *Macromolecules* **1999**, *32*, 7238.
- (10) Androsch, R.; Wunderlich, B. *Thermochim. Acta* **2000**, *364* (1–2), 181.
- (11) Schultz, J. M.; Fischer, E. W.; Schaumburg, O.; Zachmann, H. A. *J. Polym. Sci., Polym. Phys.* **1980**, *18*, 239. Strobl, G. R.; Schneider, M. J.; Voigt-Martin, I. G. *J. Polym. Sci., Polym. Phys.* **1980**, *18*, 1361.
- (12) Goderis, B.; Reynaers, H.; Scherrenberg, R.; Mathot, V. B. F.; Koch, M. H. J. *Macromolecules* **2001**, *34*, 1779.
- (13) Androsch, R.; Wunderlich, B. *Macromolecules* **2001**, *33*, 9076.
- (14) Androsch, R. *J. Therm. Anal. Calorim.* **2000**, *61* (1), 75.
- (15) Androsch, R., unpublished data.
- (16) Merzlyakov, M.; Schick, C. *Thermochim. Acta* **1999**, *330*, 55.
- (17) Androsch, R.; Moon, I.; Kreitmeier, S.; Wunderlich, B. *Thermochim. Acta* **2000**, *357–358*, 267. Androsch, R.; Wunderlich, B. *Thermochim. Acta* **2000**, *333*, 27.
- (18) Alexander, L. E. *X-Ray Diffraction Methods in Polymer Science*; Wiley: New York, 1969.
- (19) Ruland, W. *Faserforsch. Textiltech.* **1964**, *15*, 533.
- (20) Advanced Thermal Analysis System; Wunderlich, B. *Pure Appl. Chem.* **1995**, *67*, 1919. For downloadable data use WWW (Internet): <http://web.utk.edu/~athas>.

MA011118I